NEURAL REGENERATION RESEARCH
April 2017, Volume 12, Issue 4
www.nrronline.org

RESEARCH ARTICLE

Mitomycin C induces apoptosis in human epidural scar fibroblasts after surgical decompression for spinal cord injury

Tao Sui[1,#], Da-wei Ge[1,#], Lei Yang[1], Jian Tang[1], Xiao-jian Cao[1,*], Ying-bin Ge[2,*]
1 Department of Orthopedics, the First Affiliated Hospital of Nanjing Medical University, Nanjing, Jiangsu Province, China
2 Department of Physiology, Nanjing Medical University, Nanjing, Jiangsu Province, China

How to cite this article: *Sui T, Ge DW, Yang L, Tang J, Cao XJ, Ge YB (2017) Mitomycin C induces apoptosis in human epidural scar fibroblasts after surgical decompression for spinal cord injury. Neural Regen Res 12(4):644-653.*

Funding: *This research was supported by the National Natural Science Foundation of China, No. 81401791, 81371968, 81672152.*

Graphical Abstract

Whether endoplasmic reticulum stress pathway participates in mitomycin C-induced epidural scar fibroblast apoptosis?

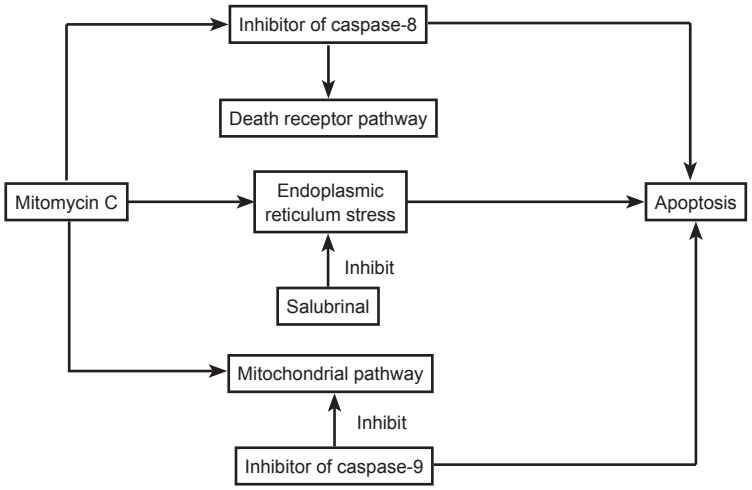

***Correspondence to:**
Xiao-jian Cao, Ph.D. or Ying-bin Ge, Ph.D., xiaojiancao001@163.com or ybge@njmu.edu.cn.

#These authors contributed equally to this study.

orcid:
0000-0003-3603-3448 (Xiao-jian Cao)
0000-0003-1471-9000 (Ying-bin Ge)

doi: *10.4103/1673-5374.205106*

Accepted: *2017-03-12*

Abstract

Numerous studies have shown that topical application of mitomycin C after surgical decompression effectively reduces scar adhesion. However, the underlying mechanisms remain unclear. In this study, we investigated the effect of mitomycin C on the proliferation and apoptosis of human epidural scar fibroblasts. Human epidural scar fibroblasts were treated with various concentrations of mitomycin C (1, 5, 10, 20, 40 μg/mL) for 12, 24 and 48 hours. Mitomycin C suppressed the growth of these cells in a dose- and time-dependent manner. Mitomycin C upregulated the expression levels of Fas, DR4, DR5, cleaved caspase-8/9, Bax, Bim and cleaved caspase-3 proteins, and it downregulated Bcl-2 and Bcl-xL expression. In addition, inhibitors of caspase-8 and caspase-9 (Z-IETD-FMK and Z-LEHD-FMK, respectively) did not fully inhibit mitomycin C-induced apoptosis. Furthermore, mitomycin C induced endoplasmic reticulum stress by increasing the expression of glucose-regulated protein 78, CAAT/enhancer-binding protein homologous protein (CHOP) and caspase-4 in a dose-dependent manner. Salubrinal significantly inhibited the mitomycin C-induced cell viability loss and apoptosis, and these effects were accompanied by a reduction in CHOP expression. Our results support the hypothesis that mitomycin C induces human epidural scar fibroblast apoptosis, at least in part, *via* the endoplasmic reticulum stress pathway.

Key Words: *nerve regeneration; spinal cord injury; mitomycin C; fibroblasts; apoptosis; endoplasmic reticulum stress; surgical decompression; epidural scar; fibrosis; CAAT/enhancer-binding protein homologous protein; glucose-regulated protein 78; neural regeneration*

Introduction

Early surgical decompression has proven to be an effective treatment after spinal cord injury (Xie et al., 2015; Bakar et al., 2016). However, postoperative epidural scar adhesion and adhesive arachnoiditis are widely accepted causes of failed back surgery syndrome, which significantly contributes to poor clinical outcomes, such as nerve radicular pain and/or low back pain (Songer et al., 1995; Robertson 1996). Therefore, it is important to prevent postoperative adhesion in spinal surgery.

Mitomycin C (MMC), a widely used chemotherapeutic drug, strongly inhibits fibroblast proliferation and prevents scar formation (Kumar et al., 2015; Na et al., 2015; Sun et al., 2015; Sui et al., 2016). Our previous experiments showed that topical application of MMC prevents epidural scar adhesion in adult rats after lumbar laminectomy, and that it was safe at low concentrations (Sun et al., 2007; Su et al., 2010).

Recently, MMC was reported to have an anti-proliferative effect by triggering the apoptotic signaling pathway in fibroblasts (Liu et al., 2010). It has been reported that intrinsic and extrinsic apoptotic pathways are both involved in MMC-induced inhibition of fibroblast proliferation (Park et al., 2000; Pirnia et al., 2002). The tumor necrosis family of proteins, including the death receptors DR4, DR5 and Fas (CD95/APO-1), which are located on the plasma membrane, have been reported to be involved in the MMC-induced apoptosis of human Tenon's fibroblasts and colon cancer cells (Hueber et al., 2002; Cheng et al., 2012). The activation of caspase-8 and caspase-9, and changes in the Bcl-2 family caused by MMC contribute to the apoptosis of human Tenon's capsule fibroblasts (Seong et al., 2005). However, the mechanism of MMC-induced apoptosis in human epidural scar fibroblasts (HESFs) differs from that in these cells, and further studies are needed.

The endoplasmic reticulum is a multifunctional organelle responsible for lipid biosynthesis, folding and exporting, vesicular traffic, protein synthesis, and cellular calcium storage (Gorman et al., 2012; Li et al., 2015). Endoplasmic reticulum stress can be triggered by various stimuli, including chemicals, oxidative stress and disturbance in Ca^{2+} homeostasis (Ron et al., 2007). Mild endoplasmic reticulum stress results in adaptation and survival involving an increase in glucose-regulated protein 78 (GRP78), while prolonged or severe endoplasmic reticulum stress leads to apoptosis involving the induction of genes, such as growth arrest and DNA damage inducible genes (GADD153 and GADD45). GADD153, also known as CAAT/enhancer-binding protein homologous protein (CHOP), is a leucine zipper transcription factor which is present at low levels in normal conditions, but is upregulated during endoplasmic reticulum stress (Wang et al., 2011). Elevated CHOP levels induce the downregulation of Bcl-2, which leads to mitochondrial dysfunction and the excessive production of reactive oxygen species, resulting in apoptosis (McCullough et al., 2001). Endoplasmic reticulum stress-induced cell death has been demonstrated in several cell lines (Zhang et al., 2012). Therefore, we hypothesized that the endoplasmic reticulum stress signaling pathway is involved in MMC-induced apoptosis of HESFs.

The primary purpose of this study was to investigate the effect of MMC on the proliferation and apoptosis of human epidural scar fibroblasts.

Materials and Methods

Materials

Primary HESFs were obtained from epidural scars after laminectomy in patients from the First Affiliated Hospital of Nanjing Medical University of China. Informed consent was acquired from all patients. This study was approved by the Ethic Committee of the First Affiliated Hospital of Nanjing Medical University in accordance with the provisions of the *Declaration of Helsinki* (No. 2010-SR-088).

Cell culture

Under sterile conditions, epidural scars were dissected into 5 mm × 5 mm pieces and dissociated in 0.25% trypsin (Gibco, Grand Island, NY, USA) for 6 minutes at 37°C. The cell suspension was centrifuged at 240 × *g* for 5 minutes. Cells were maintained in Dulbecco modified Eagle Medium (Gibco) with 10% fetal bovine serum (Gibco) and penicillin (100 U/mL)/streptomycin (100 mg/L) (Gibco) at 37°C in a humidified atmosphere of 5% CO_2 and 95% air.

MMC treatment

HESFs seeded in 24-well plates or 10-cm dishes overnight were washed with phosphate-buffered saline (PBS; pH7.4) (Keygen, Nanjing, China) and divided into MMC and control groups. Cells in the MMC group were subdivided into five subgroups according to the concentration of MMC (Kyowa Hakko Kogoyo Co., Ltd., Tokyo, Japan) used for treatment (1, 5, 10, 20 and 40 μg/mL). Cells in the control group were treated with PBS at different time points (12, 24 and 48 hours).

To further investigate the mechanism of MMC-induced apoptosis of HESFs, HESFs were pretreated with or without caspase inhibitors, including Z-IETD-FMK (20 μM, diluted in PBS) and Z-LETD-FMK (20 μM, diluted in PBS) for 2 hours. The cells were subjected to a single application of 10 μg/mL MMC (diluted in PBS) for 24 hours in the MMC group. The control group was treated with PBS for the same period. After treatment, cells were immediately washed three times with PBS for subsequent experiments.

To examine the role of endoplasmic reticulum stress in MMC-induced HESF apoptosis, the endoplasmic reticulum stress inhibitor salubrinal was used. HESFs were pretreated with or without salubrinal (10 μM) for 2 hours. Then, the cells were treated with MMC (10 μg/mL) or PBS for 24 hours in the MMC group and control group, respectively. The cells were then analyzed by Cell Counting Kit-8 (CCK-8) assay, annexin V/propidium iodide double labeling and western blot assay.

Cell viability assay

HESFs treated with various concentrations of MMC (1, 5, 10,

20 or 40 μg/mL) for 12, 24 or 48 hours were evaluated using the cell counting kit-8 assay (Dojindo Laboratories, Kumamoto, Japan) according to the manufacturer's instructions. Cells were treated with PBS in the control group. Cells were harvested and plated at a density of 1×10^4 cells/100 μL/well on a 96-well plate in 6 replicates. Cell-free culture medium was added to the blank. After 24 hours, the cells were subjected to various treatments, and then the CCK-8 solution (10 μL) was added to each well and incubated for 3–4 hours at 37°C. Thereafter, the optical density (OD) was measured at 450 nm with an absorbance microplate reader (ELx800 Absorbance Microplate Reader, Bio-Tek, USA). Cell viability (%) was equal to $(OD_{experimental\ group} - OD_{blank})/(OD_{control\ group} - OD_{blank}) \times 100\%$.

Annexin V/propidium iodide double staining

Annexin V/propidium iodide double staining (BD Biosciences, CA, USA) was used to detect cell apoptosis. HESFs were plated in 60-mm dishes (4 mL, 1×10^6/well) and incubated for 24 hours. After treatment with different concentrations of MMC, the detached and adherent cells were collected at the indicated time points and washed twice with ice-cold PBS. The cells were then resuspended in binding buffer at a concentration of 1×10^6/mL and incubated with annexin V-FITC and propidium iodide for double staining, according to the manufacturer's instructions. The mixture was incubated in the dark for 15 minutes at room temperature and analyzed using the Beckman Coulter FC500 flow cytometry system and CXP software (Beckman Coulter, Fullerton, CA,

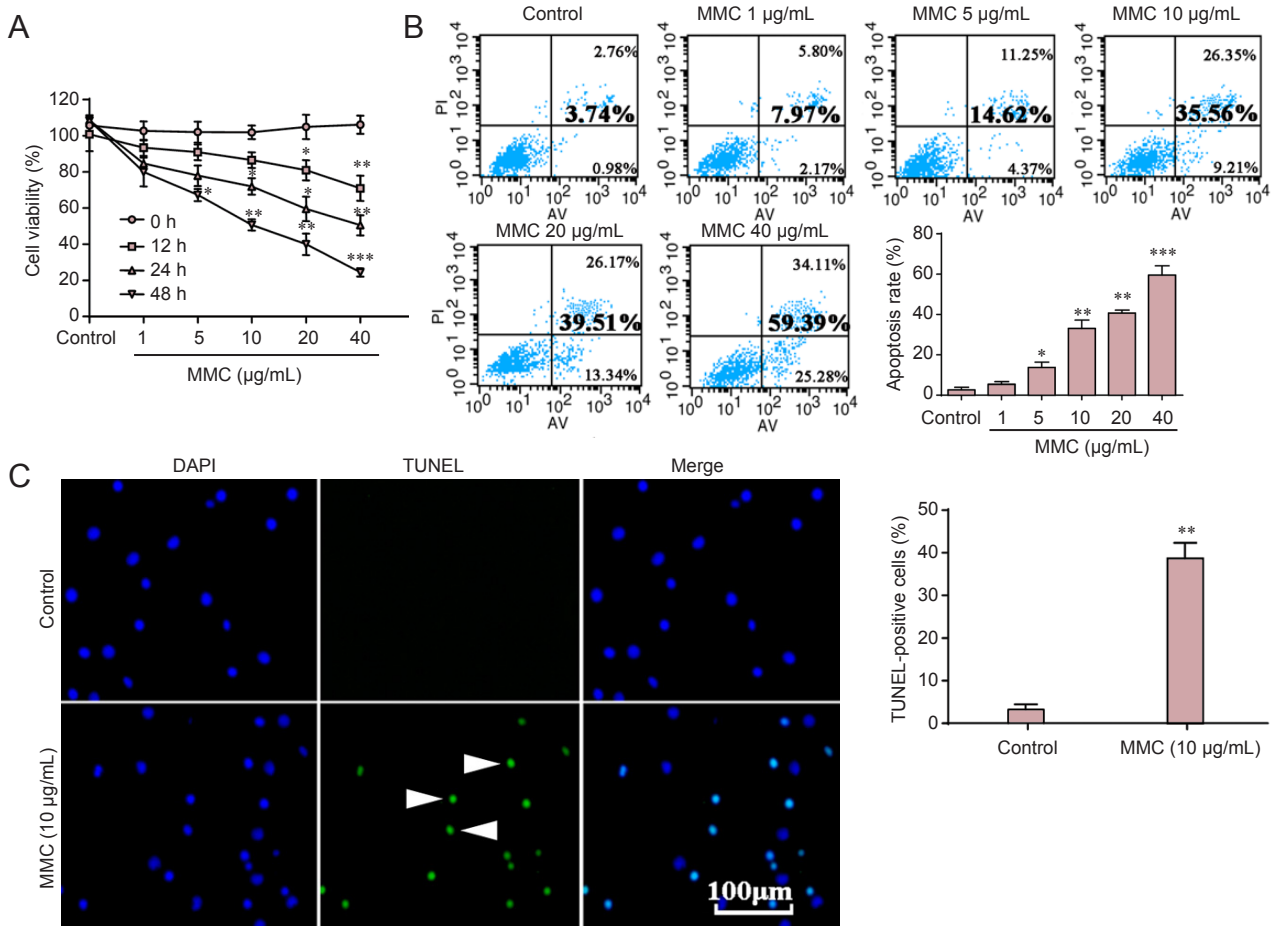

Figure 1 Effects of MMC on human epidural scar fibroblasts.

The cells shown in the bottom right quadrant were positive for annexin V-FITC and negative for propidium iodide, indicating an early stage of apoptosis. The cells in the top right quadrant stained positively for annexin V-FITC and propidium iodide, indicating that they consisted of secondary late apoptotic cells. The cells in the bottom left quadrant were normal cells, while those in the upper left quadrant were dead cells. (A) MMC induced growth inhibition in a dose-and time-dependent manner. Cell viability was evaluated using the cell counting kit-8 at the indicated time points (0, 12, 24, 48 hours) after treatment with various concentrations of MMC (1, 5, 10, 20, 40 μg/mL) or PBS. (B) Apoptosis was assessed with annexin V/propidium iodide double staining. Cells were exposed to various concentrations of MMC and PBS for 24 hours. Apoptosis rates were determined *via* flow cytometry. The total percentage of apoptotic cells is shown in bold. Statistical analysis of the total recorded apoptotic cells was performed, and the results are shown in the bar graphs. (C) Fluorescence microscopic (scale bar: 100 μm) examination of control or MMC (10 μg/mL)-treated cells for 24 hours followed by TUNEL staining (white arrowheads show positive cells). The percentage of TUNEL-positive cells was quantified and is shown by histogram. $^*P < 0.05$, $^{**}P < 0.01$, $^{***}P < 0.001$, *vs.* control group (treated with PBS). The histograms in panels A, B and C represent the mean ± SD of three independent experiments (A, B: One-way analysis of variance followed by Dunnett's *t*-test; C: Student's *t*-test). MMC: Mitomycin C; TUNEL: terminal deoxynucleotidyl transferase dUTP nick end labeling; DAPI: 4′,6-diamidino-2-phenylindole.

USA). The apoptosis rate in this study represents the total apoptosis rate, including early apoptosis rate and late apoptosis rate.

Terminal deoxynucleotidyl transferase dUTP nick end labeling (TUNEL) staining

TUNEL staining (Roche, Mannheim, Germany) was used to observe apoptotic cells. Cells were treated with 10 μg/mL MMC for 24 hours and fixed in 3.7% paraformaldehyde for 30 minutes at room temperature. After washing with PBS, the cells were incubated with blocking solution (3% H_2O_2 in methanol) for 10 minutes at 15–25°C. After rinsing with PBS, cells were permeabilized in 0.1% Triton X-100 in 0.1% sodium citrate for 2 minutes on ice, then incubated in the TUNEL reagent (green fluorescence) for 1 hour at 37°C in a humidified atmosphere in the dark and rinsed with PBS. To visualize the total number of cells in the field, slides were stained with 1 mg/L 4′,6-diamidino-2-phenylindole (blue fluorescence) (Beyotime, Hangzhou, China) for 10 minutes. Then, the apoptotic features of cells were examined by fluorescence microscopy (Olympus BX51, Tokyo, Japan). The experiment was performed in triplicate, and a minimum of 100 cells/field and at least 12 fields in each well were counted by a blind observer.

Western blot assay

HESFs were treated with 0 (control group), 5, 10 or 20 μg/mL MMC for 24 hours. Then, FAS, DR4, DR5, caspase-8, caspase-9, caspase-3 and cleaved caspase-3 protein levels were measured using western blot assay. Cells were lysed

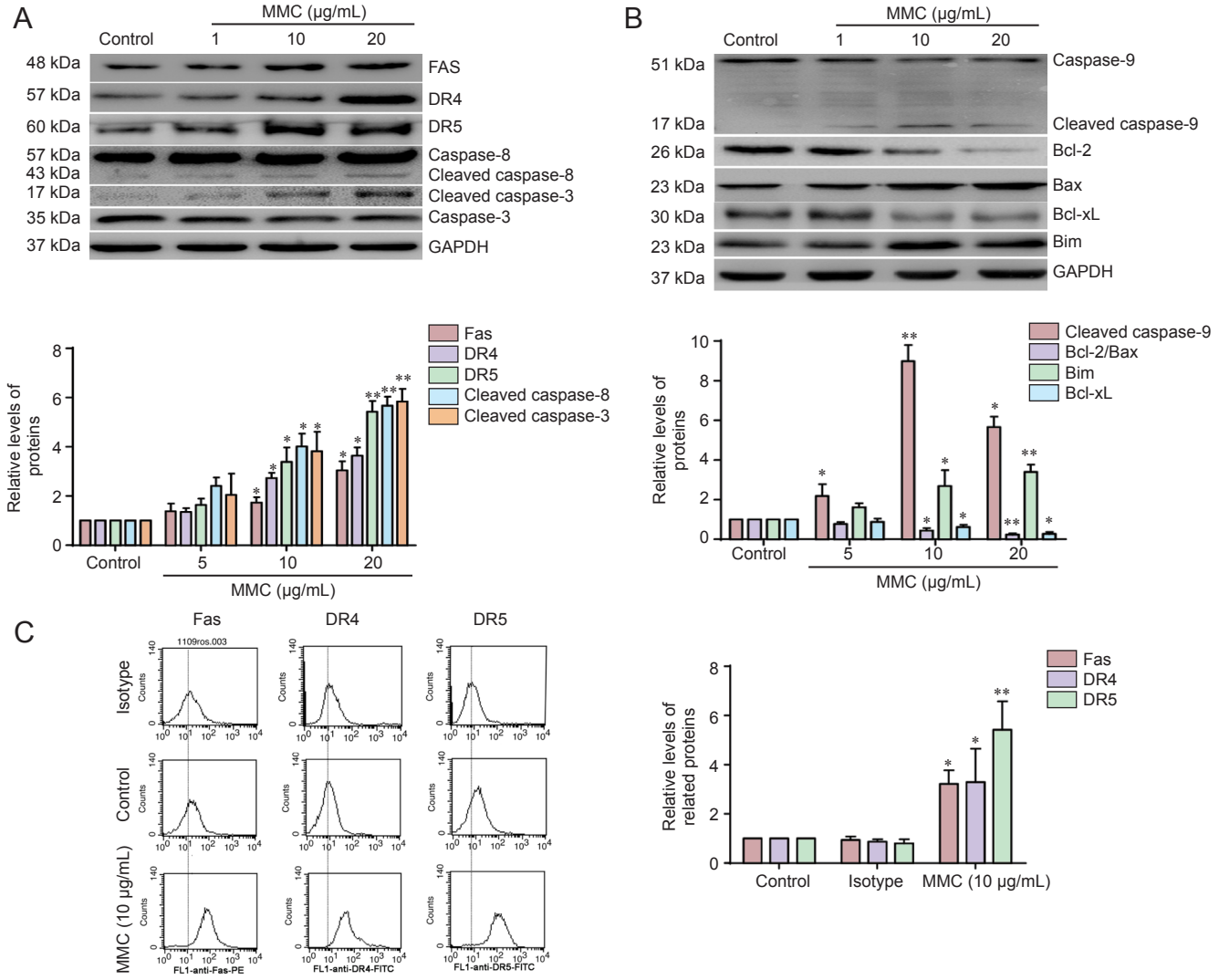

Figure 2 MMC-induced HESF apoptosis involves death receptor and mitochondrial apoptotic pathways.

HESFs were treated with various concentrations of MMC (5, 10, 20 μg/mL) or phosphate-buffered saline for 24 hours and immunoblot analysis for apoptosis-related proteins was performed. (A) Effect of MMC on death receptor apoptotic pathway associated proteins (western blot assay). (B) Effect of MMC on mitochondrial apoptotic pathway associated proteins (western blot assay). (C) HESFs were treated with 10 μg/mL MMC for 24 hours and then harvested for analysis of cell surface FAS, DR4 and DR5 by flow cytometry. The band intensities for related proteins are expressed as a histogram relative to GAPDH. The control group was normalized to a value of 1.0-fold. Data are expressed as the mean ± SD of three independent experiments. *$P < 0.05$, **$P < 0.01$, *vs.* control group (one-way analysis of variance followed by Dunnett's *t*-test). MMC: Mitomycin C; HESFs: human epidural scar fibroblasts; GAPDH: glyceraldehyde phosphate dehydrogenase.

on ice with RIPA lysis buffer (Beyotime, Hangzhou, China). Protein concentrations were determined using the Bicinchoninic Acid Protein Assay Kit (Thermo Scientific, Waltham, MA, USA). Equal amounts (25 μg/lane) of total protein were subjected to electrophoresis on 10% sodium dodecyl sulfate-polyacrylamide gels and transferred onto polyvinylidene difluoride membranes (Millipore, Bedford, MA, USA). The membranes were blocked with 5% skim milk in Tris-buffered saline and Tween 20 at room temperature for 2 hours and subsequently incubated with primary antibodies at 4°C overnight. The following primary antibodies (1:500–1:1,000) were used: mouse monoclonal FAS antibody, mouse monoclonal DR4 antibody, mouse monoclonal DR5 antibody, mouse monoclonal cleaved caspase-3 and caspase-3 antibody, mouse monoclonal cleaved caspase-8/9 and caspase-8/9 antibody (Cell Signaling Technology, Danvers, MA, USA), mouse monoclonal cleaved caspase-4 and caspase-4 antibody (MBL, Nagoya, Japan), mouse monoclonal GRP78 antibody, rabbit monoclonal CHOP antibody, rabbit polyclonal BCL-2 antibody, rabbit polyclonal Bax antibody, rabbit polyclonal Bcl-xL antibody, rabbit polyclonal Bim antibody (Cell Signaling Technology), and rabbit polyclonal GAPDH antibody (Santa Cruz Biotechnology, Santa Cruz, CA, USA). The membranes were washed three times in Tris-buffered saline and Tween 20 and incubated with horseradish peroxidase-conjugated goat anti-mouse or anti-rabbit IgG (1:5,000; Cell Signaling Technology) for 1 hour. The immune complexes were visualized by fluorography using enhanced chemiluminescence western blot detection reagents (Millipore, Bedford, USA) and visualized on X-ray films (GE, Little Chalfont, Buckinghamshire, UK). The grey value of each band was measured using Lab 2.0 Software (Bio-Rad Laboratories Inc., CA, USA). The ratio of the grey value normalized to GAPDH represents the relative concentration of the protein.

Analysis of FAS, DR4 and DR5 surface expression

Cells were treated with MMC (10 μg/mL) for 24 hours and washed with PBS supplemented with 2% fetal bovine serum after detachment by trypsinization. Cells were incubated with mouse or rabbit monoclonal anti-human FAS, DR4 or DR5 antibody (similar to the western blot assay) for 20 minutes at room temperature. Cells were then washed and incubated with FITC- or phycoerythrin-conjugated goat anti-mouse or rabbit antibody (Invitrogen, Carlsbad, CA, USA) for 20 minutes at room temperature before washing and resuspension in PBS supplemented with 2% fetal bovine serum for flow cytometric analysis (excitation wavelength of 488 nm). Samples were analyzed on a FACSCalibur flow cytometer (BD Biosciences, San Jose, CA, USA). Results were expressed as mean fluorescence intensity. Mouse and rabbit IgG isotype controls were used.

Caspase activity assay

To measure the catalytic activity of caspase family cysteine proteases, including caspase-8 and caspase-9, HESFs were lysed with a lysis buffer (1% Triton X-100, 0.32 M sucrose, 5 mM ethylenediamine tetraacetic acid, 1 mM phenylmethyl sulfonylfluoride, 1 g/mL leupeptin, 2 mM dithiothreitol, 10 mM Tris-HCl, pH 8.0) on ice for 30 minutes, and centrifuged at 16,000 × *g* for 20 minutes at 4°C. The supernatant fraction was collected and used for the assay. Caspase activity was determined using a fluorometric caspase assay kit (Promega, Madison, WI, USA) according to the manufacturer's instructions. Ac-IETD-AFC and Ac-LEHD-AFC were used as substrates for caspase-8 and caspase-9, respectively. Caspase activity was measured with a fluorescence microplate reader (Jasco FR-777, Midland, Canada) at 495 nm.

Statistical analysis

Data are presented as the mean ± SD of triplicate experiments. Statistical differences between MMC subgroups were analyzed by one-way analysis of variance followed by Dunnett's *t*-test or Student's *t*-test using SPSS 13.0 software (SPSS, Chicago, IL, USA). Statistical significance was defined at $P < 0.05$.

Results

MMC inhibited the proliferation of HESFs and induced apoptosis

Cells were treated with various concentrations of MMC (0, 1, 5, 10, 20, 40 μg/mL) for 0, 12, 24 or 48 hours and evaluated using the CCK-8 assay. As shown in **Figure 1A**, MMC inhibited the proliferation of these fibroblasts in a time- and dose-dependent manner. The IC_{50} was estimated at 10 μg/mL for the 24-hour incubation. A remarkable reduction in cell viability was observed 24 hours after treatment with MMC at a concentration of 10 μg/mL. Similar results were observed by annexin V/propidium iodide double staining. Cells treated with 0, 1, 5, 10, 20 or 40 μg/mL MMC for 24 hours underwent apoptosis in the early stage; approximately 0.98 ± 0.21%, 2.17 ± 0.94%, 4.37 ± 1.25%, 9.21 ± 3.27%, 13.34 ± 3.55% and 25.28 ± 4.59%, respectively (bottom right quadrant) (**Figure 1B**). The total percentage of apoptosis (bottom and top right quadrant) increased gradually with MMC concentration (**Figure 1B**). Additionally, to determine the cytotoxicity of MMC in HESFs, the apoptotic cells were subjected to TUNEL staining and visualized under a fluorescence microscope. As expected, the number of TUNEL-positive cells (stained with green fluorescence) significantly increased 24 hours after the treatment with 10 μg/mL MMC (**Figure 1C**). These results show that MMC inhibits HESF proliferation and induces apoptosis.

Mechanism of MMC-induced HESF apoptosis

To test whether the MMC-induced apoptosis of HESFs results from the activation of the death receptor and mitochondrial apoptotic pathways, cells were treated with 0, 5, 10 or 20 μg/mL MMC for 24 hours, and FAS, DR4, DR5, caspase-8, caspase-9, caspase-3 and cleaved caspase-3 protein levels were measured using western blot assay. As shown in **Figure 2A**, MMC-treated cells exhibited a significant upregulation in FAS, DR4, DR5 and cleaved caspase-8 levels. Furthermore, FACS analysis showed a significant upregula-

tion of cell surface receptor density for FAS, DR4 and DR5 (**Figure 2C**). This result is in accordance with the western blot assay. This finding suggests that the death receptor apoptosis pathway is involved in MMC-induced HESF apoptosis.

Immunodetection of caspase-9 showed a concentration-dependent decrease in the procaspase band and an increase in the cleaved caspase-9 band, indicating activation of caspase-9 in MMC-treated HESFs. In addition, the expression of cell survival proteins, Bcl-2 and Bcl-xL, was downregulated. In contrast, the expression of pro-apoptotic proteins, Bax and Bim, was upregulated (**Figure 2B**). In addition, the Bcl-2/Bax ratio was decreased. These results show that MMC induces HESF apoptosis through the mitochondrial pathway.

Effects of Z-IETD-FMK and Z-LETD-FMK on MMC-induced apoptosis of HESFs

To further clarify the mechanism of MMC-induced apoptosis of HESFs, we used pharmacological inhibitors of caspase-8 (Z-IETD-FMK; 20 μM) and caspase-9 (Z-LEHD-FMK; 20 μM) to test whether inhibition of these proteases impacts the cytotoxic effect of MMC on HESFs. As shown in **Figure 3A**, Z-IETD-FMK and Z-LEHD-FMK strongly decreased the corresponding caspase activity. Then, cells were pretreated with Z-IETD-FMK, Z-LEHD-FMK or a combination of these two drugs for 2 hours, and thereafter treated with 10 μg/mL MMC for 24 hours. The CCK-8 assay showed that Z-IETD-FMK and Z-LEHD-FMK pretreatment effectively increased cell viability (25.25 ± 3.45%) compared with the MMC group (**Figure 3B**). However, the combination of Z-IETD-FMK and Z-LEHD-FMK did not fully inhibit MMC-induced growth inhibition ($P < 0.05$) (**Figure 3B**). Pretreatment with Z-IETD-FMK and Z-LEHD-FMK impaired MMC-mediated apoptosis (75.24 ± 7.28%), compared with the MMC group (96.28 ± 6.32%). In addition, Z-IETD-FMK and Z-LEHD-FMK significantly diminished the MMC-induced increase in cleaved caspase-3 protein levels (**Figure 3D**). Annexin V/propidium iodide double labeling showed that in cells treated with MMC, the rate of apoptosis was 4.33% in the control group, whereas 19.99% of cells treated with Z-IETD-FMK plus Z-LEHD-FMK were apoptotic ($P < 0.05$) (**Figure 3C**). These results indicate that other apoptotic pathways might be involved in MMC-induced apoptosis in HESFs.

Effects of MMC on endoplasmic reticulum stress

Endoplasmic reticulum stress-associated apoptosis can be seen in several cell lines (Yoon et al., 2011; Wang et al., 2012). To examine whether the effects of MMC on HESFs are associated with endoplasmic reticulum stress signaling, we assessed levels of GRP78, caspase-4 and CHOP, which have been used as markers of endoplasmic reticulum stress (Gorman et al., 2012). As shown in **Figure 4A**, **B**, MMC induced a robust increase in the levels of GRP78, CHOP and cleaved caspase-4 in a dose-dependent manner (**Figure 4A**, **B**). These results indicate that endoplasmic reticulum stress is involved in MMC-induced HESF apoptosis.

Effect of salubrinal on MMC-induced HESF apoptosis

To test whether endoplasmic reticulum stress is important for MMC-induced HESF apoptosis, we used the endoplasmic reticulum stress inhibitor salubrinal. Cells were pretreated with salubrinal (10 μM) for 2 hours and then incubated with 10 μg/mL MMC for 24 hours. CCK-8 assay showed that salubrinal significantly increased cell viability compared with the MMC group (**Figure 5A**). Annexin V/propidium iodide double staining showed that in cells treated with MMC, the rate of apoptosis was 44.35 ± 5.39% in the MMC group, whereas it was only 22.88 ± 2.87% in the salubrinal pretreatment group ($P < 0.01$) (**Figure 5C**). Western blot assay showed that CHOP was significantly upregulated in MMC-treated HESFs. However, compared with the MMC group, salubrinal pretreatment downregulated CHOP protein expression (**Figure 5B**). Additionally, no difference in cell viability, apoptosis or CHOP expression levels was found between the control and salubrinal only groups. The results indicate that endoplasmic reticulum stress is involved in the MMC-induced apoptosis of HESFs.

Discussion

Excessive fibroblast proliferation following spinal cord decompression surgery plays a key role in epidural scar adhesion. Triggering apoptosis in HESFs is a promising approach for preventing postoperative epidural scar adhesion (Sun et al., 2016). The features of apoptosis (programmed cell death) include cell shrinkage, chromatin condensation, DNA fragmentation and caspase activation. Caspase-3, the most important executor of apoptosis, plays a crucial role in apoptosis (Brentnall et al., 2013; Huang, 2016; Yu et al., 2016). In the present study, CCK-8 assay showed that MMC inhibits cell proliferation in HESFs in a time- and dose-dependent manner. Annexin V/propidium iodide double staining and TUNEL staining were used to observe apoptotic cells. Higher concentrations of MMC enhanced apoptosis in HESFs. MMC increased cleaved caspase-3 protein levels. Collectively, these results demonstrate that MMC inhibits HESF proliferation and induces apoptosis in these cells.

Apoptotic signaling primarily proceeds in one of two classic apoptotic pathways—the mitochondrial pathway and the death receptor pathway (Lu et al., 2014; Wang et al., 2014). TRAIL, a member of the tumor necrosis factor superfamily, induces apoptosis through the action of the death domain receptors DR4 and DR5. It directly induces apoptosis through the extrinsic pathway, which involves activation of the initiator caspase-8, which in turn activates downstream caspases. A previous study showed that MMC upregulates cell surface expression of the TRAIL death receptors DR4 and DR5, and gene silencing of DR5 by short hairpin RNA reduces MMC-induced apoptosis (Cheng et al., 2012). A similar effect was found in our study. MMC upregulated DR4 and DR5 protein levels and cell surface receptor density. MMC induces apoptosis through activation of the Fas/FasL system or caspase cascades (with associated mitochondrial dysfunction), including the activation of caspase-9, release of cytosolic cytochrome c, and a decrease in Bcl-2 (Chang

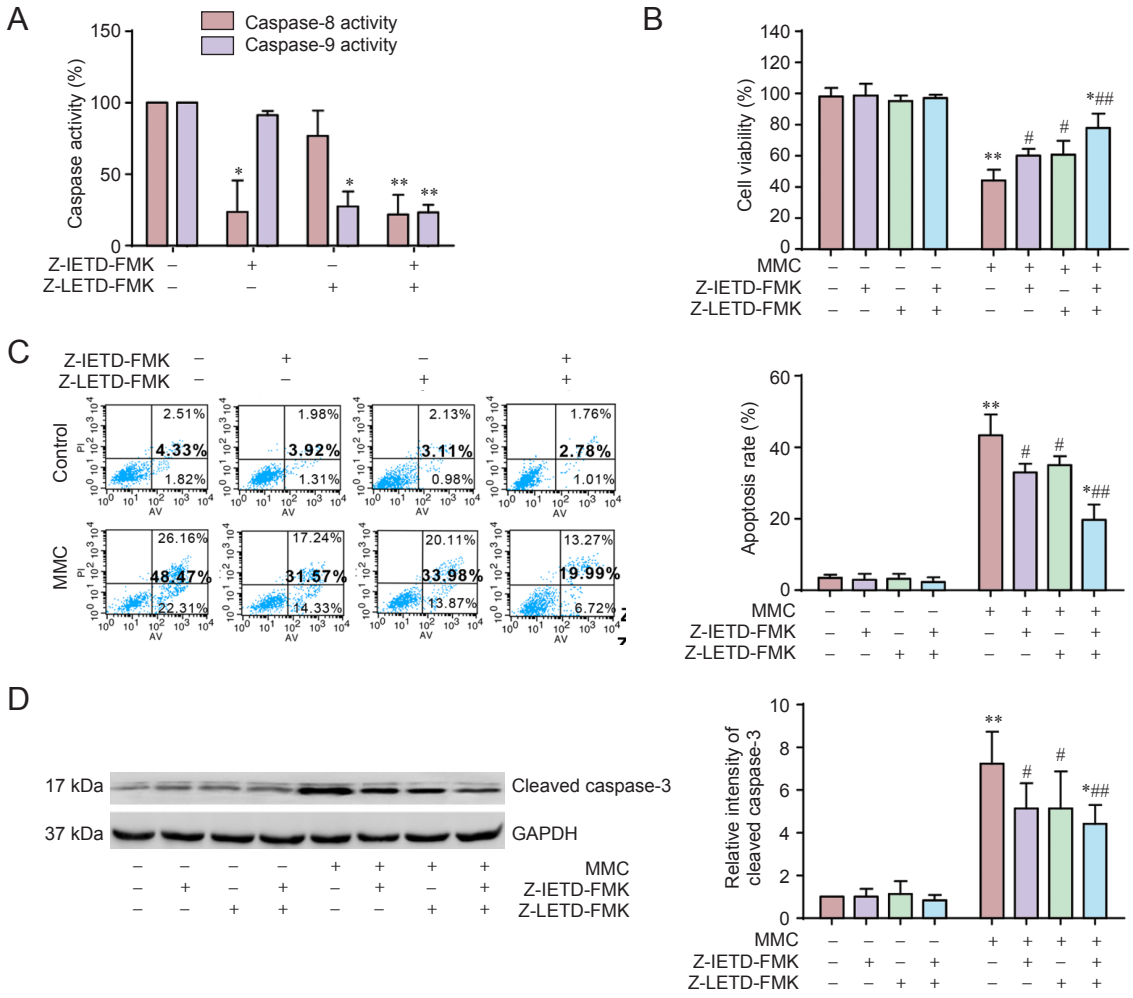

Figure 3 Z-IETD-FMK and Z-LETD-FMK partially inhibit MMC-induced apoptosis.
Cells were pretreated with Z-IETD-FMK and Z-LEHD-FMK alone or their combination for 2 hours and then treated with or without MMC (10 μg/mL) for 24 hours. (A) Catalytic activity of caspase-8 and caspase-9 was measured by cleavage of the fluorogenic biosubstrate Ac-IETD-AFC (100 μM) and Ac-LEHD-AFC (100 μM), respectively. (B) Cell viability was assessed by cell counting kit-8 assay. (C) HESF apoptosis was assessed by annexin V/propidium iodide double staining. (D) Equal amounts of whole cell lysates were analyzed by western blot assay with antibodies specific for cleaved caspase-3 and GAPDH. This experiment was performed in triplicate. The histograms represent the mean ± SD of three independent experiments (one-way analysis of variance followed by Dunnett's *t*-test). **P* < 0.05, ***P* < 0.01, *vs.* control group (phosphate buffered saline, without MMC, Z-IETD-FMK and Z-LEHD-FMK). #*P* < 0.05, ##*P* < 0.01, *vs.* the MMC group (without Z-IETD-FMK and Z-LEHD-FMK). MMC: Mitomycin C; HESFs: human epidural scar fibroblasts; GAPDH: glyceraldehyde phosphate dehydrogenase.

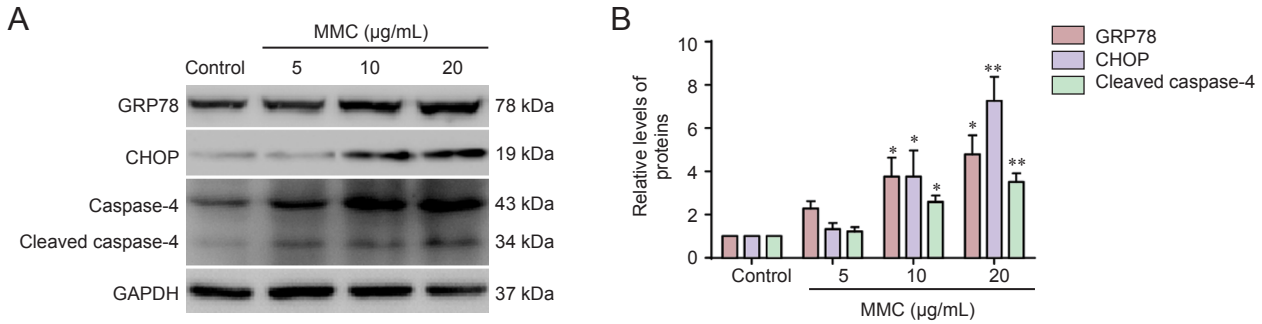

Figure 4 MMC induces endoplasmic reticulum stress.
(A) Dose-dependent effect of MMC on endoplasmic reticulum stress-associated proteins. Cells were treated with various concentrations of MMC (5, 10, 20 μg/mL) or phosphate buffered saline for 24 hours and immunoblot analysis was performed with antibodies specific for GRP78, Caspase-4, CHOP and GAPDH (control). (B) Quantitative analysis of GRP78, CHOP and cleaved caspase-4. The results are expressed as the mean ± SD of three separate experiments (A, B: one-way analysis of variance followed by Dunnett's *t*-test; C: Student's *t*-test). **P* < 0.05, ***P* < 0.01, *vs.* control group. MMC: Mitomycin C; GRP78: glucose-regulated protein 78; CHOP: CAAT/enhancer-binding protein homologous protein; GAPDH: glyceraldehyde phosphate dehydrogenase.

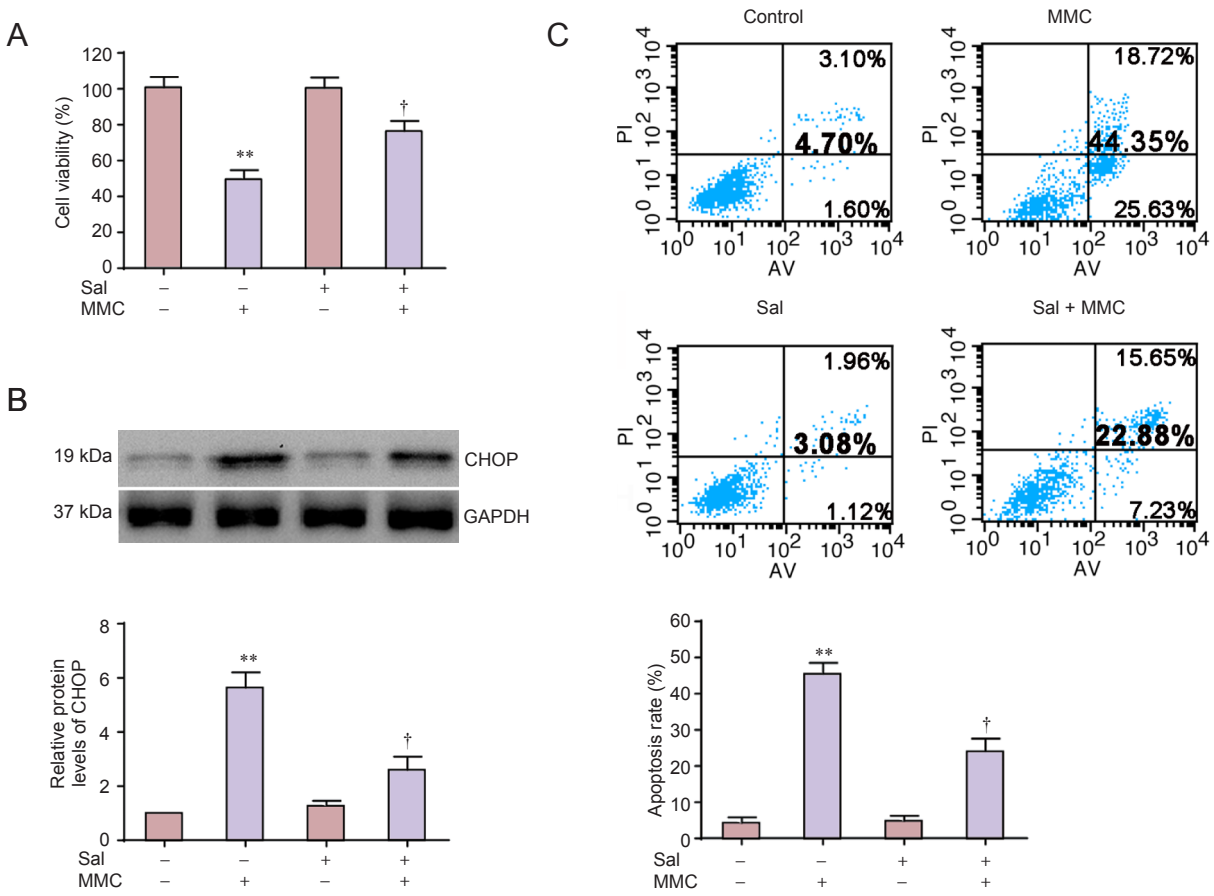

Figure 5 Sal reduces MMC-induced apoptosis in HESFs.
HESFs were pretreated with or without Sal (10 μM) for 2 hours. After treatment with MMC (10 μg/mL) or PBS for 24 hours, the cells were analyzed using a number of assays. (A) Cell viability was evaluated with the CCK-8 kit. (B) Whole-cell lysates were used for western blot assay with antibodies specific for CHOP and GAPDH (loading control). This experiment was performed in triplicate. The band intensities for CHOP were expressed as a histogram relative to GAPDH. The control group was normalized to a value of 1.0-fold. (C) Annexin V/propidium iodide double staining was performed to assess the apoptosis rate. The data in panels A, B and C are expressed as the mean ± SD of three independent experiments (one-way analysis of variance followed by Dunnett's *t*-test). $^{**}P < 0.01$, *vs.* control group (phosphate-buffered saline, without Sal or MMC). †$P < 0.05$, *vs.* HESFs treated with Sal (without MMC). Sal: Salubrinal; HESFs: human epidural scar fibroblasts; MMC: mitomycin C; GAPDH: glyceraldehyde phosphate dehydrogenase.

et al., 2010; Matsunaga et al., 2010). In our present study, MMC treatment significantly increased levels of Fas, cleaved caspase-8, cleaved caspase-9, and the pro-apoptotic proteins Bax and Bim. Furthermore, MMC treatment significantly decreased expression of the anti-apoptotic proteins Bcl-2 and Bcl-x. Collectively, these results clearly show that treatment with MMC leads to a rapid change in death receptor and mitochondrial apoptotic pathway-associated proteins. Based on these results, we speculate that MMC induces apoptosis in HESFs by the death receptor and mitochondrial pathways.

The activation of caspase-8 and caspase-9 was inhibited by Z-IETD-FMK and Z-LEHD-FMK, respectively (Pirnia et al., 2002). This result is consistent with the observation of another group (Wu et al., 2008), who reported that both Z-IETD-FMK and Z-LEHD-FMK inhibit MMC-induced apoptosis in cultured corneal endothelial cells. However, in the present study, we found that pretreatment with Z-IETD-FMK and Z-LEHD-FMK did not fully inhibit MMC-induced activation of caspase-3. In addition, MMC-mediated apoptosis was partially inhibited by caspase-8 and caspase-9 inhibitors. We hypothesize that other apoptotic pathways might be involved in the process of apoptosis induced by MMC.

Recently, the endoplasmic reticulum stress pathway was identified as a third apoptotic pathway (Binetet al., 2010; Ding et al., 2012; Yang and Hu, 2015; Sun et al., 2016). Endoplasmic reticulum stress is triggered by the alteration of endoplasmic reticulum homeostasis brought about by various pathological conditions and treatments with a variety of agents. There are three distinct signaling pathways that are triggered in response to endoplasmic reticulum stress, including Ire-1, PERK and ATF-6 (Ron and Walte, 2007). Under unstressed conditions, the luminal domains of these sensors are occupied by the endoplasmic reticulum chaperone GRP78, which inhibits their activation. During endoplasmic reticulum stress, GRP78 is released from these three transmembrane proteins, thereby activating these sensors by inducing the phosphorylation and homodimerization of PERK and IRE1 and the mobilization of ATF-6 to the Golgi for activation. Activated PERK then phosphorylates eIF2α, which causes global translational attenuation. Activation of

IRE1 initiates the nonconventional splicing of Xbp-1 mRNA and promotes the synthesis of spliced Xbp-1 protein (Treglia et al., 2012). In addition, a number of molecules, including CHOP, caspase-4 and c-Jun N-terminal kinase, are activated in endoplasmic reticulum stress. CHOP and caspase-4 are indispensable in endoplasmic reticulum stress-induced apoptosis in humans (Huang et al., 2012; Lu et al., 2014). CHOP, also known as CCAAT/enhancer-binding protein, is expressed at a low level under physiological conditions, but is strongly upregulated under endoplasmic reticulum stress. Increased expression of the transcription factor CHOP leads to the downregulation of Bcl-2 and Bim and the upregulation of Bax (Puthalakath et al., 2007; Jung et al., 2015), which may cause mitochondrial dysfunction and induce apoptosis (B'Chir et al., 2014). Additionally, CHOP knockout inhibits endoplasmic reticulum stress-induced apoptosis (Watanabe et al., 2008). Our present findings indicate that MMC induces transient increases in the levels of GRP78, CHOP and caspase-4 in a dose-dependent manner. Taken together, our results show that MMC-induced apoptosis of HESFs is coupled to endoplasmic reticulum stress.

Salubrinal, a selective inhibitor of eIF2α dephosphorylation, was found to be protective against endoplasmic reticulum stress-mediated apoptosis (Boyce et al., 2005). By inhibiting eIF2α dephosphorylation, salubrinal attenuates unfolded or misfolded protein synthesis and rescues cells from apoptosis. In neurons, salubrinal can reduce the load of mutant or mislocated proteins retained in the endoplasmic reticulum under conditions associated with neurodegeneration (Sokkaet al., 2007). Previous studies have also demonstrated that salubrinal reduces tunicamycin and hypoxia-induced apoptosis in the rat (Liu et al., 2012). Similar results were obtained in our analysis; the viability of MMC-treated HESFs was significantly increased after pretreatment with salubrinal. Salubrinal partially abrogated MMC-induced apoptosis. A recent study showed that salubrinal protects cardiomyocytes against apoptosis by downregulating the expression of CHOP and cleaved caspase-12 (Liu et al., 2012). In the present study, we assessed CHOP levels by western blot assay. Compared with the MMC-treated (without salubrinal) groups, salubrinal downregulated CHOP protein expression. This suggests that endoplasmic reticulum stress is involved in MMC-induced apoptosis.

In conclusion, we found that MMC inhibits proliferation and induces apoptosis in HESFs partially *via* the endoplasmic reticulum stress pathway. The intracellular signal transduction mechanisms remain to be clarified. MMC might have therapeutic potential for preventing excessive postoperative scarring after surgical decompression in spinal cord injury patients.

Author contributions: *XJC and YBG designed this study. TS, DWG, and JT performed experiments. TS and LY analyzed data. TS wrote the paper. All authors approved the final version of the paper.*
Conflicts of interest: *None declared.*
Plagiarism check: *This paper was screened twice using CrossCheck to verify originality before publication.*
Peer review: *This paper was double-blinded and stringently reviewed by international expert reviewers.*

References

B'Chir W, Chaveroux C, Carraro V, Averous J, Maurin A C, Jousse C, Muranishi Y, Parry L, Fafournoux P, Bruhat A (2014) Dual role for CHOP in the crosstalk between autophagy and apoptosis to determine cell fate in response to amino acid deprivation. Cell Signal 26:1385-1391.

Bakar D, Tanenbaum JE, Phan K, Alentado VJ, Steinmetz MP, Benzel EC, Mroz TE (2016) Decompression surgery for spinal metastases: a systematic review. Neurosurg Focus 41:E2.

Binet F, Chiasson S, Girard D (2010) Evidence that endoplasmic reticulum (ER) stress and caspase-4 activation occur in human neutrophils. Biochem Biophys Res Commun 391:18-23.

Boyce M, Bryant KF, Jousse C, Long K, Harding HP, Scheuner D, Kaufman RJ, Ma D, Coen DM, Ron D, Yuan J (2005) A selective inhibitor of eIF2alpha dephosphorylation protects cells from ER stress. Science 307:935-939.

Brentnall M, Rodriguez-Menocal L, De Guevara R L, Cepero E, Boise L H (2013) Caspase-9, caspase-3 and caspase-7 have distinct roles during intrinsic apoptosis. BMC Cell Biol 14:32.

Chandler K, Cappello R (2006) Laminectomy membrane formation in dogs: is the answer still elusive? Vet J 172:1-2.

Chang SW, Chou SF, Yu SY (2010) Dexamethasone reduces mitomycin C-related inflammatory cytokine expression without inducing further cell death in corneal fibroblasts. Wound Repair Regen 18:59-69.

Cheng H, Hong B, Zhou L, Allen JE, Tai G, Humphreys R, Dicker DT, Liu YY, El-Deiry WS (2012) Mitomycin C potentiates TRAIL-induced apoptosis through p53-independent upregulation of death receptors: evidence for the role of c-Jun N-terminal kinase activation. Cell Cycle 11:3312-3323.

Ding W, Yang L, Zhang M, Gu Y (2012) Reactive oxygen species-mediated endoplasmic reticulum stress contributes to aldosterone-induced apoptosis in tubular epithelial cells. Biochem Biophys Res Commun 418:451-456.

Gorman AM, Healy SJ, Jager R, Samali A (2012) Stress management at the ER: regulators of ER stress-induced apoptosis. Pharmacol Ther 134:306-316.

Gotoh T, Oyadomari S, Mori K, Mori M (2002) Nitric oxide-induced apoptosis in RAW 264.7 macrophages is mediated by endoplasmic reticulum stress pathway involving ATF6 and CHOP. J Biol Chem 277:12343-12350.

Grassner L, Wutte C, Klein B, Mach O, Riesner S, Panzer S, Vogel M, Bühren V, Strowitzki M, Vastmans J, Maier D (2016) Early decompression (< 8 h) after traumatic cervical spinal cord injury improves functional outcome as assessed by spinal cord independence measure after one year. J Neurotrauma 33:1658-1666.

Huang W (2016) Neuroprotective effect of tamoxifen in a model rat with aucte spinal cord injury. Zhongguo Zuzhi Gongcheng Yanjiu 20:7710-7716.

Huang X, Li L, Zhang L, Zhang Z, Wang X, Zhang X, Hou L, Wu K (2012) Crosstalk between endoplasmic reticulum stress and oxidative stress in apoptosis induced by alpha-tocopheryl succinate in human gastric carcinoma cells. Br J Nutr 7:1-9.

Hueber A, Welsandt G, Jordan JF, Mietz H, Weller M, Krieglstein GK, Esser PJ (2002) Characterization of CD95 ligand (CD95L)-induced apoptosis in human tenon fibroblasts. Exp Eye Res 75:1-8.

Jung KJ, Min KJ, Bae JH, Kwon TK (2015) Carnosic acid sensitized TRAIL-mediated apoptosis through down-regulation of c-FLIP and Bcl-2 expression at the post translational levels and CHOP-dependent up-regulation of DR5, Bim, and PUMA expression in human carcinoma caki cells. Oncotarget 6:1556-1568.

Kumar V, Ali MJ, Ramachandran C (2015) Effect of mitomycin-C on contraction and migration of human nasal mucosa fibroblasts: implications in dacryocystorhinostomy. Br J Ophthalmol 99:1295-1300.

Li HF, Zhao SX, Xing BP, Sun ML (2015) Ulinastatin suppresses endoplasmic reticulum stress and apoptosis in the hippocampus of rats with acute paraquat poisoning. Neural Regen Res 10:467-472.

Liu CL, Li X, Hu GL, Li RJ, He YY, Zhong W, Li S, He KL, Wang LL (2012) Salubrinal protects against tunicamycin and hypoxia induced cardiomyocyte apoptosis via the PERK-eIF2alpha signaling pathway. J Geriatr Cardiol 9:258-268.

Liu J, Ni B, Zhu L, Yang J, Cao X, Zhou W (2010) Mitomycin C-polyethylene glycol controlled-release film inhibits collagen secretion and induces apoptosis of fibroblasts in the early wound of a postlaminectomy rat model. Spine J 10:441-447.

Lu M, Lawrence DA, Marsters S, Acosta-Alvear D, Kimmig P, Mendez AS, Paton AW, Paton JC, Walter P, Ashkenazi A (2014) Opposing unfolded-protein-response signals converge on death receptor 5 to control apoptosis. Science 345:98-101.

Lu TH, Tseng TJ, Su CC, Tang FC, Yen CC, Liu YY, Yang CY, Wu CC, Chen KL, Hung DZ, Chen YW (2014) New insights into the roles of CHOP-induced apoptosis in ER stress. Toxicol Lett 224:130-140.

Matsunaga T, Tsuji Y, Kaai K, Kohno S, Hirayama R, Alpers DH, Komoda T, Hara A (2010) Toxicity against gastric cancer cells by combined treatment with 5-fluorouracil and mitomycin C: implication in oxidative stress. Cancer Chemother Pharmacol 66:517-526.

Matsuyama S, Reed JC (2000) Mitochondria-dependent apoptosis and cellular pH regulation. Cell Death Differ 7:1155-1165.

McCullough KD, Martindale JL, Klotz LO, Aw TY, Holbrook NJ (2001) Gadd153 sensitizes cells to endoplasmic reticulum stress by down-regulating Bcl2 and perturbing the cellular redox state. Mol Cell Biol 21:1249-1259.

Na JH, Sung KR, Shin JA, Moon JI (2015) Antifibrotic effects of pirfenidone on Tenon's fibroblasts in glaucomatous eyes: comparison with mitomycin C and 5-fluorouracil. Graefes Arch Clin Exp Ophthalmol 253:1537-1545.

Oyadomari S, Mori M (2004) Roles of CHOP/GADD153 in endoplasmic reticulum stress. Cell Death Differ 11:381-389.

Pan G, O'Rourke K, Chinnaiyan AM, Gentz R, Ebner R, Ni J, Dixit VM (1997) The receptor for the cytotoxic ligand TRAIL. Science 276:111-113.

Park IC, Park MJ, Hwang CS, Rhee CH, Whang DY, Jang JJ, Choe TB, Hong SI, Lee SH (2000) Mitomycin C induces apoptosis in a caspases-dependent and Fas/CD95-independent manner in human gastric adenocarcinoma cells. Cancer Lett 158:125-132.

Pirnia F, Schneider E, Betticher DC, Borner MM (2002) Mitomycin C induces apoptosis and caspase-8 and -9 processing through a caspase-3 and Fas-independent pathway. Cell Death Differ 9:905-914.

Puthalakath H, O'Reilly LA, Gunn P, Lee L, Kelly PN, Huntington ND, Hughes PD, Michalak EM, McKimm-Breschkin J, Motoyama N, Gotoh T, Akira S, Bouillet P, Strasser A (2007) ER stress triggers apoptosis by activating BH3-only protein Bim. Cell 129:1337-1349.

Robertson JT (1996) Role of peridural fibrosis in the failed back: a review. Eur Spine J 5 Suppl 1:S2-6.

Ron D, Walter P (2007) Signal integration in the endoplasmic reticulum unfolded protein response. Nat Rev Mol Cell Biol 8:519-529.

Seong GJ, Park C, Kim CY, Hong YJ, So HS, Kim SD, Park R (2005) Mitomycin-C induces the apoptosis of human Tenon's capsule fibroblast by activation of c-Jun N-terminal kinase 1 and caspase-3 protease. Invest Ophthalmol Vis Sci 46:3545-3552.

Shi K, Wang D, Cao X, Ge Y (2013) Endoplasmic reticulum stress signaling is involved in mitomycin C (MMC)-induced apoptosis in human fibroblasts via PERK pathway. PLoS One 8:e59330.

Sokka AL, Putkonen N, Mudo G, Pryazhnikov E, Reijonen S, Khiroug L, Belluardo N, Lindholm D, Korhonen L (2007) Endoplasmic reticulum stress inhibition protects against excitotoxic neuronal injury in the rat brain. J Neurosci 27:901-908.

Songer MN, Rauschning W, Carson EW, Pandit SM (1995) Analysis of peridural scar formation and its prevention after lumbar laminotomy and discectomy in dogs. Spine (Phila Pa 1976) 20:571-580.

Su C, Yao C, Lu S, Zhang A, Cao X, Teng G, Zang F (2010) Study on the optimal concentration of topical mitomycin-C in preventing postlaminectomy epidural adhesion. Eur J Pharmacol 640:63-67.

Sui T, Liu L, Wu XT, Cao XJ (2016) Local application of mitomycin C for prevention of epidural fibrosis: study protocol for a prospective randomized controlled double-blinded trial. Clin Trials Orthop Disord 1:22-30.

Sun GZ, Gao FF, Zhao ZM, Sun H, Xu W, Wu LW, He YC (2016) Endoplasmic reticulum stress-induced apoptosis in the penumbra aggravates secondary damage in rats with traumatic brain injury. Neural Regen Res 11:1260-1266.

Sun Y, Ge Y, Fu Y, Yan L, Cai J, Shi K, Cao X, Lu C (2015) Mitomycin C induces fibroblasts apoptosis and reduces epidural fibrosis by regulating miR-200b and its targeting of RhoE. Eur J Pharmacol 765:198-208.

Sun Y, Wang LX, Wang L, Sun SX, Cao XJ, Wang P, Feng L (2007) A comparison of the effectiveness of mitomycin C and 5-fluorouracil in the prevention of peridural adhesion after laminectomy. J Neurosurg Spine 7:423-428.

Sun Y, Zhao S, Li X, Yan L, Wang J, Wang D, Chen H, Dai J, He J (2016) Local application of rapamycin reduces epidural fibrosis after laminectomy via inhibiting fibroblast proliferation and prompting apoptosis. J Orthop Surg Res 11:58.

Tajiri S, Oyadomari S, Yano S, Morioka M, Gotoh T, Hamada JI, Ushio Y, Mori M (2004) Ischemia-induced neuronal cell death is mediated by the endoplasmic reticulum stress pathway involving CHOP. Cell Death Differ 11:403-415.

Treglia AS, Turco S, Ulianich L, Ausiello P, Lofrumento DD, Nicolardi G, Miele C, Garbi C, Beguinot F, Di Jeso B (2012) Cell fate following ER stress: just a matter of "quo ante" recovery or death? Histol Histopathol 27:1-12.

Wang F, Song W, Brancati G, Segatori L (2011) Inhibition of endoplasmic reticulum-associated degradation rescues native folding in loss of function protein misfolding diseases. J Biol Chem 286:43454-43464.

Wang WJ, Wang Y, Chen HZ, Xing YZ, Li FW, Zhang Q, Zhou B, Zhang HK, Zhang J, Bian XL, Li L, Liu Y, Zhao BX, Chen Y, Wu R, Li AZ, Yao LM, Chen P, Zhang Y, Tian XY, et al. (2014) Orphan nuclear receptor TR3 acts in autophagic cell death via mitochondrial signaling pathway. Nat Chem Biol 10:133-140.

Wang Y, Wan B, Li D, Zhou J, Li R, Bai M, Chen F, Yu L (2012) BRSK2 is regulated by ER stress in protein level and involved in ER stress-induced apoptosis. Biochem Biophys Res Commun 423:813-818.

Watanabe Y, Tsuchiya H, Sakabe T, Matsuoka S, Akechi Y, Fujimoto Y, Yamane K, Ikeda R, Nishio R, Terabayashi K, Ishii K, Gonda K, Matsumi Y, Ashla AA, Okamoto H, Takubo K, Tomita A, Hoshikawa Y, Kurimasa A, Itamochi H, et al. (2008) CD437 induces apoptosis in ovarian adenocarcinoma cells via ER stress signaling. Biochem Biophys Res Commun 366:840-847.

Wu KY, Wang HZ, Hong SJ (2008) Mechanism of mitomycin-induced apoptosis in cultured corneal endothelial cells. Mol Vis 14:1705-1712.

Xie JB, Zhang X, Li QH, Xu ZJ (2015) Inhibition of inflammatory cytokines after early decompression may mediate recovery of neurological function in rats with spinal cord injury. Neural Regen Res 10:219-224.

Yang JW, Hu ZP (2015) Neuroprotective effects of atorvastatin against cerebral ischemia/reperfusion injury through the inhibition of endoplasmic reticulum stress. Neural Regen Res 10:1239-1244.

Yoon H, Kim DS, Lee GH, Kim KW, Kim HR, Chae HJ (2011) Apoptosis induced by manganese on neuronal SK-N-MC cell line: endoplasmic reticulum (er) stress and mitochondria dysfunction. Environ Health Toxicol 26:e2011017.

Yu SW, Andrabi SA, Wang H, Kim NS, Poirier GG, Dawson TM, Dawson VL (2006) Apoptosis-inducing factor mediates poly (ADP-ribose) (PAR) polymer-induced cell death. Proc Natl Acad Sci U S A 103:18314-18319.

Yu YQ, Hu NC, Duan JA, Li DP, Liu C (2016) Neuroprotective effects of sufentanil preconditioning on spinal cord injury in mouse models. Zhongguo Zuzhi Gongcheng Yanjiu 20:5966-5972.

Zhang R, Piao MJ, Kim KC, Kim AD, Choi JY, Choi J, Hyun JW (2012) Endoplasmic reticulum stress signaling is involved in silver nanoparticles-induced apoptosis. Int J Biochem Cell Biol 44:224-232.

Copyedited by Patel B, Pack M, Wang J, Li CH, Qiu Y, Song LP, Zhao M